Chinese Physics C

PAPER • OPEN ACCESS

Quasi-two-body $B_{(s)} \to K^*\gamma \to K\pi\gamma$ decays in the perturbative QCD approach*

To cite this article: Zhi-Qing Zhang *et al* 2022 *Chinese Phys. C* **46** 123105

Quasi-two-body $B_{(s)} \to K^*\gamma \to K\pi\gamma$ decays in the perturbative QCD approach*

Zhi-Qing Zhang(张志清)† Yan-Chao Zhao(赵彦超) Zhi-Lin Guan(关志林) Zhi-Jie Sun(孙志杰)
Zi-Yu Zhang(张梓於) Ke-Yi He(何珂依)

Department of Physics, Henan University of Technology, Zhengzhou 450052, China

Abstract: In this study, we investigate quasi-two-body $B_{(s)} \to K^*\gamma \to K\pi\gamma$ decays in the perturbative QCD approach. Two-meson distribution amplitudes are introduced to describe the final state interactions of the $K\pi$ pair, which involve time-like form factors and Gegenbauer polynomials. We calculate the *CP* averaged branching ratios of the $B_{(s)} \to K^*\gamma \to K\pi\gamma$ decays. Our results are in agreement with newly updated data measured by Belle II. This suggests that it is more appropriate to analyze these quasi-two-body *B* decays in the three-body framework than the two-body framework. We also predict direct *CP* asymmetries for the considered decay modes and find that $A_{CP}(B_{u,d} \to K^*\gamma \to K\pi\gamma)$ is small and less than 1% in magnitude, whereas $A_{CP}(B_s \to K^*\gamma \to K\pi\gamma)$ is larger and can reach a few percent. Our predictions can be tested in future *B* meson experiments.

Keywords: *B* meson decay, perturbative QCD, three-body radiative decay

DOI: 10.1088/1674-1137/ac89d1

I. INTRODUCTION

Many experimental studies on three-body *B* meson decays [1–9] have been performed in recent years. This type of decay has gained increasing attention for the following reasons. (1) Many new resonance states are observed in the invariant mass distributions of three-body decays, which are difficult to understand in terms of a common meson or baryon and are known as exotic states. Researchers are puzzled by their inner structures and have proposed numerous assumptions, such as compact $qq\bar{q}\bar{q}$ tetraquarks, $qqqq\bar{q}$ pentaquarks, loosely bound hadronic molecules, and glueball and hybrid states. (2) These decays involve significantly more complicated QCD dynamics compared with two-body decay cases, which imposes a serious challenge to present theoretical frameworks. The hard *b*-quark decay kernels in three-body *B* decays contain two virtual gluons at the leading order, which are difficult to directly evaluate owing to the enormous number of Feynman diagrams. (3) Large direct *CP* asymmetries in the localized regions of phase spaces for three-body *B* decays have been observed in experiments. For three-body *B* decays, *CP* violation depends on the invariant mass, and regional *CP* asymmetries can be measured through the Dalitz plot. However, such observables do not exist in two-body *B* decays. To study these three-body *B* decays, many approaches based on symmetry principles and factorization theorems have been proposed. Symmetry principles include U-spin [10–13], flavor $SU(3)$ symmetry [14–17], and the factorization-assisted topological-diagram amplitude (FAT) approach [18]. Factorization theorems include the QCD-improved factorization approach [19– 24] and perturbative QCD (PQCD) approach [25–34], and it has been proposed that the factorization theorem of three-body *B* decays is approximately valid when two energetic final particles move collinearly and the bachelor particle recoils back. At the same time, the interactions between them can be neglected. Based on this quasi-two-body-decay approximation, two-meson distribution amplitudes (DAs) are introduced into the PQCD approach, where the strong dynamics between the two final hadrons in the resonant regions are included.

On the experimental side, the $B^{0,+} \to K^{*0,+}\gamma$ decays have recently been investigated by Belle II [35], and their branching ratios were obtained through different decay modes.

Received 5 July 2022; Accepted 16 August 2022; Published online 24 August 2022

* Supported in part by the National Natural Science Foundation of China under (11347030), the Program of Science and Technology Innovation Talents in Universities of Henan Province (14HASTIT037)

† E-mail: zhangzhiqing@haut.edu.cn

$$Br\left(B^0 \to K^{*0}[K^+\pi^-]\gamma\right) = (4.5 \pm 0.3 \pm 0.2) \times 10^{-5},$$
$$Br\left(B^0 \to K^{*0}[K^0\pi^0]\gamma\right) = (4.4 \pm 0.9 \pm 0.6) \times 10^{-5},$$
$$Br\left(B^+ \to K^{*+}[K^+\pi^0]\gamma\right) = (5.0 \pm 0.5 \pm 0.4) \times 10^{-5},$$
$$Br\left(B^+ \to K^{*+}[K^0\pi^+]\gamma\right) = (5.4 \pm 0.6 \pm 0.4) \times 10^{-5}. \quad (1)$$

The two-body $B^{0,+} \to K^{*0,+}\gamma$ decays have been studied using different theories, including the PQCD approach [36–38]. Here, we study three-body radiative B decays in the quasi-two-body approximation using the PQCD approach. Verifying the consistency between the three-body and two-body analyses of the $B_{(s)} \to K^*\gamma \to K\pi\gamma$ decays can support PQCD factorization for exclusive B meson decays. Furthermore, by studying these more subtle channels compared with two-body decays, we can deepen our understanding of isospin symmetry and the narrow width approximation involved in these decays. After introducing the new non-perturbative inputs, the two-meson DAs, the factorization formula for the three-body B decay $B \to h_1 h_2 h_3$ can be written as [39, 40]

$$\mathcal{M} = \Phi_B \otimes H \otimes \Phi_{h_1 h_2} \otimes \Phi_{h_3}, \quad (2)$$

where $\Phi_B(\Phi_{h_3})$ denotes the $B(h_3)$ meson DA, $\Phi_{h_1 h_2}$ is the two-meson DA for $h_1 h_2$ that fly collinearly, and $\otimes$ represents the convolution in parton momenta. Then, the hard kernel H for the b quark decay, similar to the two-body decay case, starts with the diagrams of single hard gluon exchange.

This paper is organized as follows. In Sec. II, the kinematic variables for three-body radiative B decays are defined. The considered two-meson ($K\pi$) P-wave DAs are parametrized, whose normalization form factors are assumed to follow the relativistic Breit-Wigner (RBW) model. Then, Feynman diagrams and the total decay amplitudes for these channels are given. In Sec. III, the numerical results are presented and discussed, where we compare our predictions with other theoretical and experimental results. The summary is presented in the final section.

II. FRAMEWORK

We begin with the parametrization of the kinematic variables involved in the $B \to K^*\gamma \to K\pi\gamma$ decays. In the rest frame of the B meson, we define the B meson momentum P_B, K meson momentum P_1, π meson momentum P_2, K^* meson momentum $P = P_1 + P_2$, and γ momentum P_3 in light-cone coordinates as

$$P_B = \frac{m_B}{\sqrt{2}}(1,1,0_T), P = \frac{m_B}{\sqrt{2}}(1,\eta,0_T), P_3 = \frac{m_B}{\sqrt{2}}(0,1-\eta,0_T),$$

$$P_1 = \frac{m_B}{\sqrt{2}}(\zeta,(1-\zeta)\eta,P_{1T}), \quad P_2 = \frac{m_B}{\sqrt{2}}((1-\zeta),\zeta\eta,P_{2T}), \quad (3)$$

where m_B is the B meson mass, the variable $\eta = P^2/m_B^2 = \omega^2/m_B^2$, ω is the invariant mass of the $K\pi$ pair, and ζ is the momentum fraction for the K meson. The momenta of the light quarks in the B and K^* mesons are denoted as k_B and k, respectively,

$$k_B = \left(0, \frac{m_B}{\sqrt{2}}x_1, k_{1T}\right), \quad k = \left(\frac{m_B}{\sqrt{2}}z, 0, k_{2T}\right), \quad (4)$$

where x_1 and z are the momentum fractions.

A. Distribution amplitudes

Because the massless photon is only transversely polarized, only the transversely polarized P-wave DAs of the $K\pi$ pair contribute to the final results, which are defined as [30]

$$\Phi^T_{K\pi}(z,\zeta,\omega) = \frac{1}{\sqrt{2N_c}}\Big[\gamma_5 \not{\epsilon}_T \not{p} \phi^T_{K\pi}\left(z,\omega^2\right) + \omega\gamma_5 \not{\epsilon}_T \phi^a_{K\pi}\left(z,\omega^2\right) + \mathrm{i}\omega \frac{\epsilon^{\mu\nu\rho\sigma}\gamma_\mu \epsilon_{T\nu} p_\rho n_{-\sigma}}{p\cdot n_-}\phi^v_{K\pi}\left(z,\omega^2\right)\Big]\sqrt{\zeta(1-\zeta)}, \quad (5)$$

with the functions [41]

$$\phi^T_{K\pi}(z,\omega^2) = \frac{3F^\perp_{K\pi}(\omega^2)}{\sqrt{2N_c}}z(1-z) \times \left[1 + a^\perp_{1K^*}3t + a^\perp_{2K^*}\frac{3}{2}(5t^2-1)\right],$$
$$\phi^a_{K\pi}(z,\omega^2) = \frac{3F^\parallel_{K\pi}(\omega^2)}{4\sqrt{2N_c}}t,$$
$$\phi^v_{K\pi}(z,\omega^2) = \frac{3F^\parallel_{K\pi}(\omega^2)}{8\sqrt{2N_c}}(1+t^2), \quad (6)$$

where $t = (1-2z)$, and the Gegenbauer moments associated with the transverse polarization $a^\perp_{1K^*}, a^\perp_{2K^*}$ are determined in Ref. [34] and are listed in the next section.

The strong interactions between the resonance and final-state meson pair can be factorized into a time-like form factor, which is guaranteed by the Watson theorem [42]. For narrow resonances, the RBW [43] function is a convenient model to effectively separate them from other resonant and nonresonant contributions with the same spin and has been widely used in experimental data analyses. Here, the time-like form factor $F^\parallel_{K\pi}(\omega^2)$ is parametrized with the RBW line shape and can be expressed in the following form [44, 45]:

$$F^{\parallel}_{K\pi}(\omega^2) = \frac{m^2_{K^*}}{m^2_{K^*} - \omega^2 - \mathrm{i} m_{K^*}\Gamma_{K^*}(\omega^2)}, \tag{7}$$

where m_{K^*} and $\Gamma_{K^*}(\omega^2)$ are the pole mass and width, respectively. The mass dependent width $\Gamma_{K^*}(\omega^2)$ is defined as

$$\Gamma_{K^*}(\omega^2) = \Gamma_{K^*}\left(\frac{m_{K^*}}{\omega}\right)\left(\frac{|\overrightarrow{P_1}|}{|\overrightarrow{P_0}|}\right)^{(2L_R+1)} \frac{1+(|\overrightarrow{P_0}|r_{BW})^2}{1+(|\overrightarrow{P_1}|r_{BW})^2}, \tag{8}$$

where $|\overrightarrow{P_1}|$ is the magnitude of the $K(\pi)$ momentum measured in the resonance K^* rest frame, whereas $|\overrightarrow{P_0}|$ is the value of $|\overrightarrow{P_1}|$ corresponding to $\omega = m_{K^*}$. L_R is the orbital angular momentum in the $K\pi$ system, and $L_R = 1$ corresponds to the P-wave resonances. Owing to limited studies on the form factor $F^{\perp}_{K\pi}(\omega^2)$, we use the two decay constants $f^T_{K^*}$ and f_{K^*} of the intermediate particle to determine this factor through the ratio $F^{\perp}_{K\pi}(\omega^2)/F^{\parallel}_{K\pi}(\omega^2) \approx (f^T_{K^*}/f_{K^*})$ [27]. Note that this approximation is workable in the region with $\omega^2 \approx m^2_{K^*}$.

For the wave function of the heavy $B_{(s)}$ meson [46], we take

$$\Phi_{B_{(s)}}(x,b) = \frac{1}{\sqrt{2N_c}}\left(P\!\!\!/_{B_{(s)}} + m_{B_{(s)}}\right)\gamma_5 \phi_{B_{(s)}}(x,b). \tag{9}$$

Here, only the contribution of the Lorentz structure $\phi_{B_{(s)}}(x,b)$ is considered because the contribution of the second Lorentz structure $\bar{\phi}_{B_{(s)}}$ is numerically small and has previously been neglected [47]. For the distribution amplitude $\phi_{B_{(s)}}(x,b)$ in Eq. (9), we adopt the following model:

$$\phi_{B_{(s)}}(x,b) = N_{B_{(s)}} x^2(1-x)^2 \exp\left(-\frac{x^2 m^2_{B_{(s)}}}{2\omega_b^2} - \frac{\omega_b^2 b^2}{2}\right), \tag{10}$$

where the shape parameter $\omega_b = 0.40 \pm 0.04$ ($\omega_b = 0.50 \pm 0.05$) GeV is well fixed using rich experimental data on the $B_{(s)}$ meson from many studies, and the coefficient $N_{B_{(s)}}$ is determined by the normalization $\int_0^1 \mathrm{d}x \phi_{B_{(s)}}(x, b=0) = 1$. An updated discussion on the B meson wave function can be found in Ref. [48].

B. Analytic formulae

For quasi-two-body $B \to K^*\gamma \to K\pi\gamma$ decays, the effective Hamiltonian relevant to the $b \to s$ transition is given by [49]

$$H_{\rm eff} = \frac{G_{\rm F}}{\sqrt{2}}\Bigg[\sum_{q=u,c} V_{qb}V^*_{qs}\{C_1(\mu)O_1^{(q)}(\mu) + C_2(\mu)O_2^{(q)}(\mu)\} - \sum_{i=3\sim 8g} V_{tb}V^*_{ts}C_i(\mu)O_i(\mu)\Bigg] + \text{H.c.}, \tag{11}$$

where the Fermi coupling constant $G_{\rm F} \simeq 1.166\times 10^{-5}$ GeV^{-2} [50], and $V_{qb}V^*_{qs}$ and $V_{tb}V^*_{ts}$ are the products of the Cabibbo-Kobayashi-Maskawa (CKM) matrix elements. The scale μ separates the effective Hamiltonian into two distinct parts: the Wilson coefficients C_i and local four-quark operators O_i. The local four-quark operators are written as

$$\begin{aligned}
O_1^{(q)} &= (\bar{s}_i q_j)_{V-A}(\bar{q}_j b_i)_{V-A},\\
O_2^{(q)} &= (\bar{s}_i q_i)_{V-A}(\bar{q}_j b_j)_{V-A},\\
O_3 &= (\bar{s}_i b_i)_{V-A}\sum_q(\bar{q}_j q_j)_{V-A},\\
O_4 &= (\bar{s}_i b_j)_{V-A}\sum_q(\bar{q}_j q_i)_{V-A},\\
O_5 &= (\bar{s}_i b_i)_{V-A}\sum_q(\bar{q}_j q_j)_{V+A},\\
O_6 &= (\bar{s}_i b_j)_{V-A}\sum_q(\bar{q}_j q_i)_{V+A},\\
O_7 &= \frac{3}{2}(\bar{s}_i b_i)_{V-A}\sum_q e_q(\bar{q}_j q_j)_{V+A},\\
O_8 &= \frac{3}{2}(\bar{s}_i b_j)_{V-A}\sum_q e_q(\bar{q}_j q_i)_{V+A},\\
O_9 &= \frac{3}{2}(\bar{s}_i b_i)_{V-A}\sum_q e_q(\bar{q}_j q_j)_{V-A},\\
O_{10} &= \frac{3}{2}(\bar{s}_i b_j)_{V-A}\sum_q e_q(\bar{q}_j q_i)_{V-A},\\
O_{7\gamma} &= \frac{e}{8\pi^2} m_b \bar{s}_i \sigma^{\mu\nu}(1+\gamma_5)b_i F_{\mu\nu},\\
O_{8g} &= \frac{g}{8\pi^2} m_b \bar{s}_i \sigma^{\mu\nu}(1+\gamma_5)T^a_{ij} b_j G^a_{\mu\nu},
\end{aligned} \tag{12}$$

with the color indices i and j. Here, $V \pm A$ refer to the Lorentz structures $\gamma_\mu(1\pm\gamma_5)$. Note that the terms associated with the strange quark mass in the $O_{7\gamma}$ and O_{8g} operators are dropped.

The typical Feynman diagrams at the leading order for quasi-two-body $B \to K^*\gamma \to K\pi\gamma$ decays are shown in Figs. 1–5, where we take the $B \to K^{*0}\gamma \to K^0\pi^0\gamma$ decay as an example. The contributions from the $O_{7\gamma}, O_{8g}, O_2$ operators and the annihilation type diagrams are presented, and the analytic formulas for the decay amplitudes of each Feynman diagram can be found in our previous paper [32]. The wave functions and corresponding parameters must be replaced in the calculations.

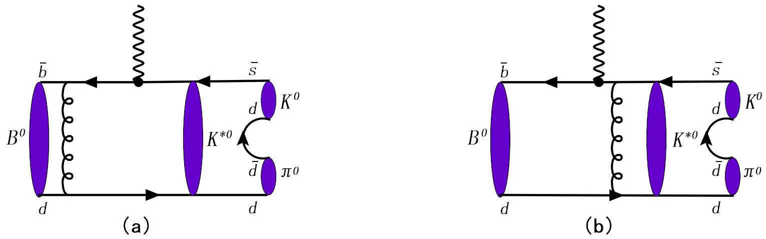

Fig. 1. (color online) Feynman diagrams from the operator $O_{7\gamma}$.

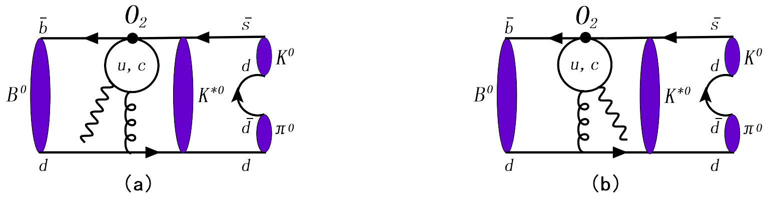

Fig. 2. (color online) Quark-loop diagrams from the operator O_2 with the photon being emitted from the quark loop.

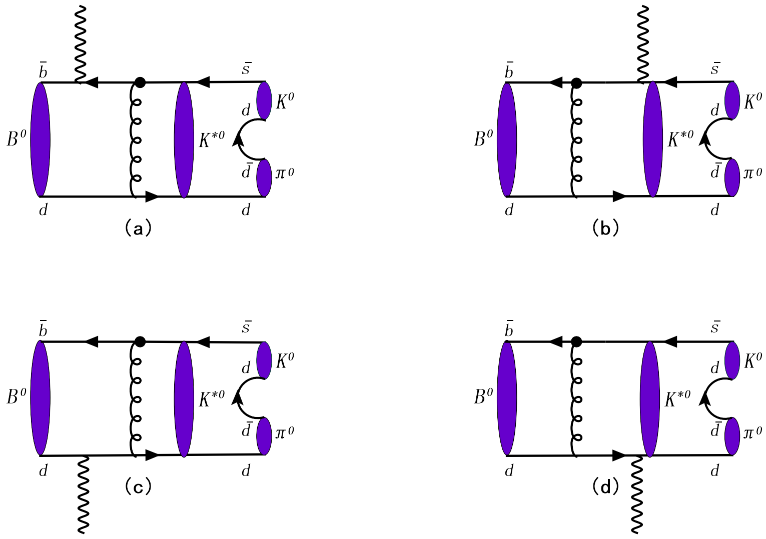

Fig. 3. (color online) Feynman diagrams from the operator O_{8g}.

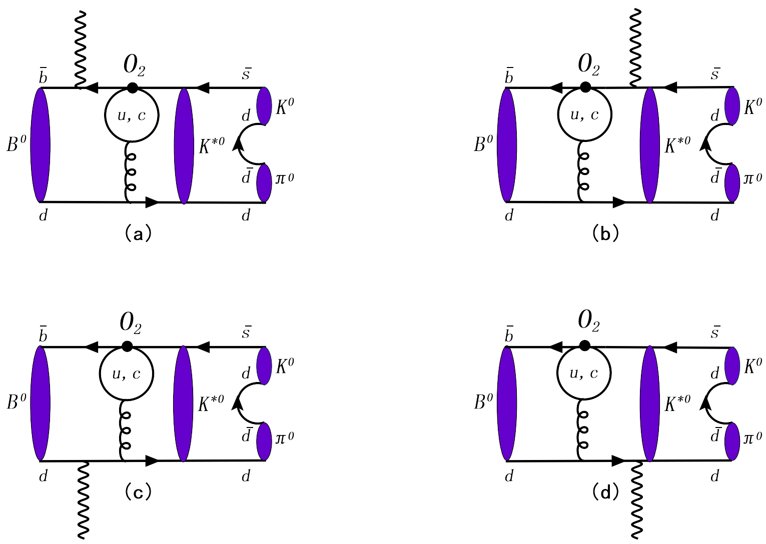

Fig. 4. (color online) Quark-loop diagrams from the operator O_2 with a photon being emitted by an external quark.

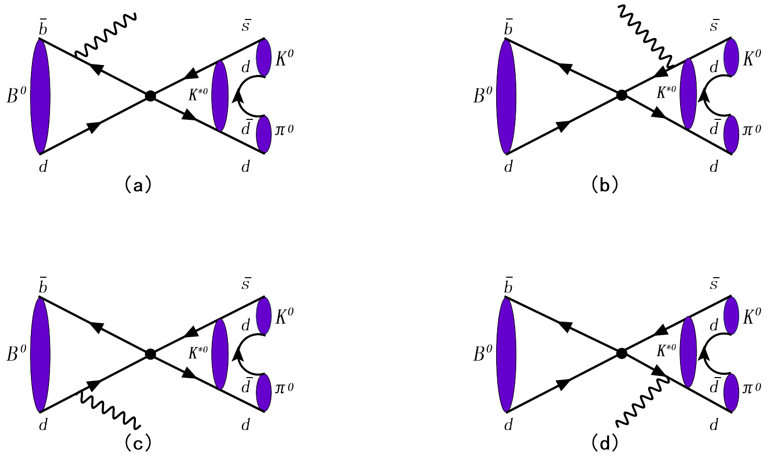

Fig. 5. (color online) Annihilation diagrams.

By combining the amplitudes from the different Feynman diagrams, the total decay amplitude of the charged B meson decay is given as

$$\begin{aligned}\mathcal{A}^i(B^+) =& \frac{G_F}{\sqrt{2}} V_{ub}^* V_{us} \Big\{ C_2 \left(\mathcal{M}_{1u}^{i(a)} + \mathcal{M}_{1u}^{i(b)}(Q_u) + \mathcal{M}_{2u}^{i} \right) \\ &+ a_1 \left(\mathcal{M}_{ann}^{i(a,LL)}(Q_u) + \mathcal{M}_{ann}^{i(b,LL)}(Q_u) \right) \Big\} \\ &+ \frac{G_F}{\sqrt{2}} V_{cb}^* V_{cs} \left\{ C_2 \left(\mathcal{M}_{1c}^{i(a)} + \mathcal{M}_{1c}^{i(b)}(Q_u) + \mathcal{M}_{2c}^{i} \right) \right\} \\ &- \frac{G_F}{\sqrt{2}} V_{tb}^* V_{ts} \Big\{ C_{7\gamma} \mathcal{M}_{7\gamma}^{i} + C_{8g} \left(\mathcal{M}_{8g}^{i(a)} + \mathcal{M}_{8g}^{i(b)}(Q_u) \right) \\ &+ (a_4 + a_{10}) \left(\mathcal{M}_{ann}^{i(a,LL)}(Q_u) + \mathcal{M}_{ann}^{i(b,LL)}(Q_u) \right) \\ &+ (a_6 + a_8) \mathcal{M}_{ann}^{i(SP)}(Q_u) \Big\},\end{aligned} \tag{13}$$

where $i = R, L$ correspond to contributions from the right-handed and left-handed photons, respectively, and the combinations of the Wilson coefficients are defined as

$$\begin{aligned}a_1 =& C_2 + C_1/3, \quad a_4 = C_4 + C_3/3, \quad a_6 = C_6 + c_5/3, \\ a_8 =& C_8 + C_7/3, \quad a_{10} = C_{10} + C_9/3.\end{aligned} \tag{14}$$

Similarly, the total decay amplitudes for the $B^0_{(s)} \to K^*\gamma \to K\pi\gamma$ decays are listed below.

$$\begin{aligned}\mathcal{A}^i(B^0) =& \frac{G_F}{\sqrt{2}} V_{ub}^* V_{us} \left\{ C_2 \left(\mathcal{M}_{1u}^{i(a)} + \mathcal{M}_{1u}^{i(b)}(Q_d) + \mathcal{M}_{2u}^{i} \right) \right\} \\ &+ \frac{G_F}{\sqrt{2}} V_{cb}^* V_{cs} \left\{ C_2 \left(\mathcal{M}_{1c}^{i(a)} + \mathcal{M}_{1c}^{i(b)}(Q_d) + \mathcal{M}_{2c}^{i} \right) \right\} \\ &- \frac{G_F}{\sqrt{2}} V_{tb}^* V_{ts} \Big\{ C_{7\gamma} \mathcal{M}_{7\gamma}^{i} + C_{8g} \left(\mathcal{M}_{8g}^{i(a)} + \mathcal{M}_{8g}^{i(b)}(Q_d) \right) \\ &+ (a_4 - \frac{1}{2} a_{10}) \left(\mathcal{M}_{ann}^{i(a,LL)}(Q_d) + \mathcal{M}_{ann}^{i(b,LL)}(Q_d) \right) \\ &+ (a_6 - \frac{1}{2} a_8)\, \mathcal{M}_{ann}^{i(SP)}(Q_d) \Big\},\end{aligned} \tag{15}$$

$$\begin{aligned}\mathcal{A}^i(B_s^0) =& \frac{G_F}{\sqrt{2}} V_{ub}^* V_{ud} \left\{ C_2 \left(\mathcal{M}_{1u}^{i(a)} + \mathcal{M}_{1u}^{i(b)}(Q_s) + \mathcal{M}_{2u}^{i} \right) \right\} \\ &+ \frac{G_F}{\sqrt{2}} V_{cb}^* V_{cd} \left\{ C_2 \left(\mathcal{M}_{1c}^{i(a)} + \mathcal{M}_{1c}^{i(b)}(Q_s) + \mathcal{M}_{2c}^{i} \right) \right\} \\ &- \frac{G_F}{\sqrt{2}} V_{tb}^* V_{td} \Big\{ C_{7\gamma} \mathcal{M}_{7\gamma}^{i} + C_{8g} \left(\mathcal{M}_{8g}^{i(a)} + \mathcal{M}_{8g}^{i(b)}(Q_s) \right) \\ &+ (a_4 - \frac{1}{2} a_{10}) \left(\mathcal{M}_{ann}^{i(a,LL)}(Q_s) + \mathcal{M}_{ann}^{i(b,LL)}(Q_s) \right) \\ &+ (a_6 - \frac{1}{2} a_8)\, \mathcal{M}_{ann}^{i(SP)}(Q_s) \Big\}.\end{aligned} \tag{16}$$

Then, the differential decay rate can be described as

$$\frac{d\mathcal{B}}{d\omega^2} = \tau_B \frac{|\overrightarrow{P_1}||\overrightarrow{P_3}|}{64\pi^3 m_B^3} \sum_{i=R,L} |\mathcal{A}^i|^2, \tag{17}$$

where the squared amplitudes for the $B_{(s)}$ meson decays are summed in the helicity basis, τ_B is the mean lifetime of the $B_{(s)}$ meson, and the kinematic variables $|\overrightarrow{P_1}|$ and $|\overrightarrow{P_3}|$ denote the magnitudes of the K and γ momenta in the center-of-mass frame of the $K\pi$ pair,

$$\begin{aligned}|\overrightarrow{P_1}| =& \frac{1}{2} \sqrt{[(\omega^2 - (m_K + m_\pi)^2)(\omega^2 - (m_K - m_\pi)^2)]/\omega^2}, \\ |\overrightarrow{P_3}| =& \frac{1}{2}(m_B^2 - \omega^2)/\omega.\end{aligned} \tag{18}$$

III. NUMERICAL RESULTS

The adopted input parameters in our numerical calculations are summarized below (the masses, decay constants, Gegenbauer moments, and QCD scale are in units of GeV, whereas the B meson lifetimes are in units of ps) [50–52].

$$\Lambda_{\rm QCD}=0.25,\ m_{B^+}=5.279,\ m_{B^0}=5.280,\ m_{B_s}=5.267,$$
$$m_b=4.8,\ m_{K^\pm}=0.494,\ m_{K^0}=0.498,\ m_{\pi^\pm}=0.140,$$
$$m_{\pi^0}=0.135,\ m_{K^{*0}}=0.89555,\ m_{K^{*\pm}}=0.89176,\ f_B=0.19,$$
$$f_{B_s}=0.23,\ \tau_{B^+}=1.638,\ \tau_{B^0}=1.520,\ \tau_{B_s^0}=1.509,$$
$$\Gamma_{K^{*0}}=47.3,\ \Gamma_{K^{*\pm}}=50.3,\ r_{BW}=4{\rm GeV}^{-1},\ f_{K^*}=0.217,$$
$$f_{K^*}^T=0.185,\ a_{1K^*}^\perp=0.31\pm0.16,\ a_{2K^*}^\perp=1.188\pm0.098. \tag{19}$$

As for the CKM matrix elements, we employ Wolfenstein parametrization with the inputs [50]

$$\lambda=0.22453\pm0.00044,\quad A=0.836\pm0.015,$$
$$\bar\rho=0.122^{+0.018}_{-0.017},\quad \bar\eta=0.355^{+0.012}_{-0.011}. \tag{20}$$

Using the differential branching ratio in Eq. (17) and the squared amplitudes in Eqs. (13) and (15) and integrating over the full $K\pi$ invariant mass region $(m_K+m_\pi)\leq\omega\leq M_{B_{(s)}}$ for the resonant components, we obtain the branching ratios of the quasi-two-body decays as

$$Br\left(B^0\to K^{*0}\gamma\to K^+\pi^-\gamma\right)=\left(3.08^{+1.29+0.33+0.24+0.12}_{-0.86-0.30-0.36-0.08}\right)\times10^{-5},$$
$$Br\left(B^0\to K^{*0}\gamma\to K^0\pi^0\gamma\right)=\left(1.55^{+0.64+0.16+0.12+0.06}_{-0.44-0.15-0.19-0.04}\right)\times10^{-5},$$
$$Br\left(B^+\to K^{*+}\gamma\to K^+\pi^0\gamma\right)=\left(1.72^{+0.67+0.20+0.08+0.10}_{-0.46-0.17-0.12-0.07}\right)\times10^{-5},$$
$$Br\left(B^+\to K^{*+}\gamma\to K^0\pi^+\gamma\right)=\left(3.21^{+1.25+0.36+0.20+0.15}_{-0.87-0.31-0.23-0.12}\right)\times10^{-5}, \tag{21}$$

where the first source of errors originates from the shape parameter of the B meson DA, $\omega_B=0.4\pm0.04$ GeV, the second error is from the Gegenbauer coefficients in the kaon-pion DAs, $a_{1K^*}^\perp=0.31\pm0.16$ GeV, $a_{2K^*}^\perp=1.188\pm$ 0.098 GeV, and the final two errors are induced by next-to-leading-order effects in the PQCD approach, that is, changing the hard scale t from 0.80t to 1.2t and the QCD scale $\Lambda_{\rm QCD}=0.25\pm0.05$ GeV. From our results, we can see that the dominant theoretical error arises from the uncertainty on ω_B, which is close to 40%. The error induced by the Gegenbauer coefficients in the $K\pi$ pair DAs is smaller at approximately 10%. These four decays are mediated by the $b\to s$ transition. In our calculations, the Feynman diagrams from the operator $O_{7\gamma}$ give the dominant contribution, which is proportional to $V_{tb}V_{ts}^*\sim\lambda^2$.

Assuming isospin conservation for the strong decay $K^*\to K\pi$, we can obtain the following relations:

$$\frac{\Gamma(K^{*0}\to K^+\pi^-)}{\Gamma(K^{*0}\to K\pi)}=2/3,\quad \frac{\Gamma(K^{*0}\to K^0\pi^0)}{\Gamma(K^{*0}\to K\pi)}=1/3,$$
$$\frac{\Gamma(K^{*+}\to K^0\pi^+)}{\Gamma(K^{*+}\to K\pi)}=2/3,\quad \frac{\Gamma(K^{*+}\to K^+\pi^0)}{\Gamma(K^{*+}\to K\pi)}=1/3. \tag{22}$$

Under the narrow width approximation, the branching ratios of these quasi-two-body decays can be expressed as

$$Br\left(B^0\to K^{*0}\gamma\to K^+\pi^-\gamma\right)$$
$$=Br(B^0\to K^{*0}\gamma)\cdot Br(K^{*0}\to K^+\pi^-),$$
$$Br\left(B^0\to K^{*0}\gamma\to K^0\pi^0\gamma\right)$$
$$=Br(B^0\to K^{*0}\gamma)\cdot Br(K^{*0}\to K^0\pi^0),$$
$$Br\left(B^+\to K^{*+}\gamma\to K^+\pi^0\gamma\right)$$
$$=Br(B^+\to K^{*+}\gamma)\cdot Br(K^{*+}\to K^+\pi^0),$$
$$Br\left(B^+\to K^{*+}\gamma\to K^0\pi^+\gamma\right)$$
$$=Br(B^+\to K^{*+}\gamma)\cdot Br(K^{*+}\to K^0\pi^+). \tag{23}$$

Using the experimental data given in Eq. (1), which were measured by Belle II in the last year, combined with isospin conservation (Eq. (22)) and the narrow width approximation (Eq. (23)), we can estimate the branching ratios of the quasi-two-body decays as follows:

$$Br\left(B^0\to K^{*0}\gamma\to K^+\pi^-\gamma\right)=(3.00\pm0.20\pm0.13)\times10^{-5},$$
$$Br\left(B^0\to K^{*0}\gamma\to K^0\pi^0\gamma\right)=(1.47\pm0.30\pm0.20)\times10^{-5},$$
$$Br\left(B^+\to K^{*+}\gamma\to K^+\pi^0\gamma\right)=(1.67\pm0.17\pm0.13)\times10^{-5},$$
$$Br\left(B^+\to K^{*+}\gamma\to K^0\pi^+\gamma\right)=(3.60\pm0.40\pm0.27)\times10^{-5}. \tag{24}$$

These estimates and our predictions are consistent with each other; therefore, it is reasonable to extend the PQCD approach to quasi-two-body B meson decays.

Using the numerical results given with Eq. (21), we calculate the relative ratios $R_{1,2}$ between the branching ratios of the charged and neutral B decays,

$$R_1=\frac{Br\left(B^+\to K^{*+}\gamma\to K^0\pi^+\gamma\right)}{Br\left(B^0\to K^{*0}\gamma\to K^+\pi^-\gamma\right)}=1.04^{+0.63}_{-0.46},$$
$$R_2=\frac{Br\left(B^+\to K^{*+}\gamma\to K^+\pi^0\gamma\right)}{Br\left(B^0\to K^{*0}\gamma\to K^0\pi^0\gamma\right)}=1.11^{+0.67}_{-0.49}. \tag{25}$$

If we assume the branching ratio of the decay $K^*\to K\pi$ to be 100% and the narrow width approximation to be true, we can relate them with the ratio $R=\dfrac{Br(B^+\to K^{*+}\gamma)}{Br(B^0\to K^{*0}\gamma)}$. Using data from PDG [50], the ratio

$R = \dfrac{Br(B^+ \to K^{*+}\gamma)}{Br(B^0 \to K^{*0}\gamma)} = 0.94 \pm 0.08$ can be obtained. Using the updated data measured by Belle II [35], the ratio $R = \dfrac{Br(B^+ \to K^{*+}\gamma)}{Br(B^0 \to K^{*0}\gamma)} = 1.16 \pm 0.14$. The values of theseratios once again support the usability and rationality of PQCD factorization for quasi-two-body B decays. Furthermore, we can relate these ratios with isospin asymmetry, which is defined as

$$A_I = \frac{\Gamma(B^0 \to K^{*0}\gamma) - \Gamma(B^+ \to K^{*+}\gamma)}{\Gamma(B^0 \to K^{*0}\gamma) - \Gamma(B^+ \to K^{*+}\gamma)}. \tag{26}$$

This can be rewritten using the formula $Br = \tau_B \Gamma/\hbar$

$$A_I = \frac{1 - \frac{\tau_{B^0}}{\tau_{B^+}} Br(B^+ \to K^{*+}\gamma)/Br(B^0 \to K^{*0}\gamma)}{1 + \frac{\tau_{B^0}}{\tau_{B^+}} Br(B^+ \to K^{*+}\gamma)/Br(B^0 \to K^{*0}\gamma)} = \frac{1 - \frac{\tau_{B^0}}{\tau_{B^+}} R}{1 + \frac{\tau_{B^0}}{\tau_{B^+}} R}. \tag{27}$$

The ratios $R_{1,2}$ suggest that isospin asymmetry between the decays $B^+ \to K^{*+}\gamma$ and $B^0 \to K^{*0}\gamma$ is small at approximately 2 % in magnitude, which is supported by the present data. The branching ratios of the two-body $B^{+,0} \to K^{*+,0}\gamma$ decays have previously been calculated with the PQCD approach [37], where the results were $Br(B^0 \to K^{*0}\gamma) = (5.2 \pm 2.6) \times 10^{-5}, Br(B^+ \to K^{*+}\gamma) = (5.3 \pm 2.7) \times 10^{-5}$. Two years later, they were updated to $Br(B^0 \to K^{*0}\gamma) = (3.81^{+1.73+0.55+0.11}_{-1.27-0.38-0.11}) \times 10^{-5}, Br(B^+ \to K^{*+}\gamma) = (3.58^{+1.76+0.54+0.11}_{-1.28-0.40-0.11}) \times 10^{-5}$ [53]. Comparing these two calculations, differences still exist. A comparison of all the theoretical results with the updated data measured by Belle II supports the idea that it is more appropriate to study these quasi-two-body B decays in the three-body framework than the two-body framework. Under the times of high precision measurement, these results should be carefully tested in LHCb experiments.

Using the same two-meson DAs for the $K\pi$ pair, we also calculate the branching ratios for the $B_s^0 \to \bar{K}^{*0}\gamma \to K^0\pi^0(K^-\pi^+)\gamma$ decays and obtain the results as

$$Br\left(B_s^0 \to \bar{K}^{*0}\gamma \to \bar{K}^0\pi^0\gamma\right) = \left(0.35^{+0.16+0.04+0.00+0.02}_{-0.11-0.03-0.02-0.02}\right) \times 10^{-6},$$
$$Br\left(B_s^0 \to \bar{K}^{*0}\gamma \to K^-\pi^+\gamma\right) = \left(0.69^{+0.33+0.08+0.00+0.04}_{-0.21-0.07-0.03-0.03}\right) \times 10^{-6}. \tag{28}$$

These two decays are induced by the $b \to d$ transition, whose penguin contributions are proportional to $V_{tb}V_{td}^* \sim \lambda^3$ and expected to be suppressed by one order of magnitude relative to those induced by the $b \to s$ transition. From Eq. (28), we can obtain $Br(B_s \to \bar{K}^{*0}\gamma) = (1.04^{+0.51}_{-0.34}) \times 10^{-6}$ through the $\bar{K}^{*0} \to K^-\pi^+$ internal decay mode and $(1.05^{+0.50}_{-0.35}) \times 10^{-6}$ through $\bar{K}^{*0} \to \bar{K}^0\pi^0$. Our predictions are consistent with the results given in Ref. [53]

$$Br\left(B_s^0 \to \bar{K}^{*0}\gamma\right) = \left(1.11^{+0.42+0.15+0.16}_{-0.32-0.12-0.07}\right) \times 10^{-6}. \tag{29}$$

The consistency of these results indicates that the PQCD approach is applicable to two-body and three-body B decays at the same time.

We also predict the ω−dependences of the $B^+ \to K^{*+}\gamma \to K^+\pi^0\gamma$ and $B_s \to \bar{K}^{*0}\gamma \to K^-\pi^+\gamma$ decay spectra shown in Fig. 6, which exhibit a maximum at the $K\pi$ invariant mass at approximately 0.895 GeV. The curves for the other four B decay modes are similar because the same time-like form factors are used for the $K\pi$ DAs. It is easy to see that the main contribution to the branching ratio originates from the region around the pole mass of the K^* resonance, as expected. For example, the central values of the branching ratio $BR(B^+ \to K^{*+}\gamma \to K^+\pi^0\gamma)$ are 0.89×10^{-5} and 1.30×10^{-5} when we integrate over ω by limiting the ranges of $\omega = [m_{K^*} - 0.5\Gamma_{K^*}, m_{K^*} + 0.5\Gamma_{K^*}]$ and $\omega = [m_{K^*} - \Gamma_{K^*}, m_{K^*} + \Gamma_{K^*}]$, repectively. These amount to 52 % and 76 % of the total branching ratio $Br(B^+ \to K^{*+}\gamma \to K^+\pi^0\gamma) = 1.72 \times 10^{-5}$, respectively.

The direct CP asymmetry of $B_{(s)} \to K^*\gamma \to K\pi\gamma$ is defined as

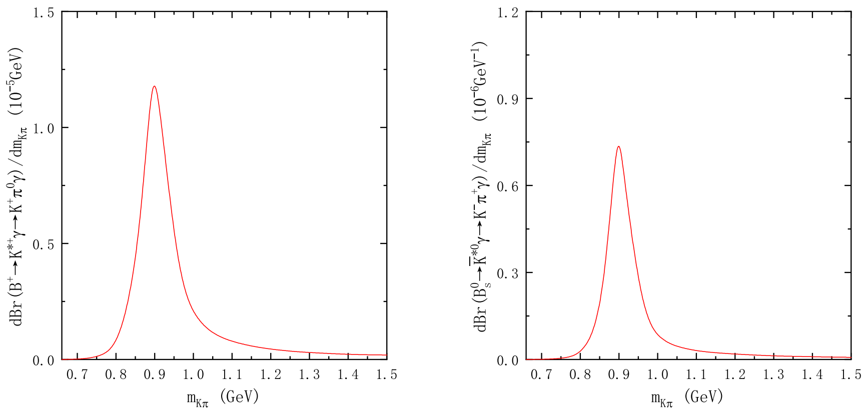

Fig. 6. (color online) Predicted $B^+ \to K^{*+}\gamma \to K^+\pi^0\gamma$ (left) and $B_s \to \bar{K}^{*0}\gamma \to K^-\pi^+\gamma$ (right) decay spectra in the $K\pi$ invariant mass.

$$A_{CP} = \frac{\Gamma\left(\bar{B}_{(s)} \to \bar{K}^*\gamma \to \overline{(K\pi)}\gamma\right) - \Gamma\left(B_{(s)} \to K^*\gamma \to K\pi\gamma\right)}{\Gamma\left(\bar{B}_{(s)} \to \bar{K}^*\gamma \to \overline{(K\pi)}\gamma\right) + \Gamma\left(B_{(s)} \to K^*\gamma \to K\pi\gamma\right)}. \tag{30}$$

For our considered decays, direct CP asymmetry is mainly induced by interference between the contributions from the $O_{7\gamma}$ and tree operators, which is proportional to $V_{ub}^* V_{us(d)}$. We predict the direct CP asymmetries as

$$\begin{aligned}
&A_{CP}\left(B^0 \to K^{*0}\gamma \to K^+\pi^-\gamma\right)\\
&=\left(-0.58^{+0.04+0.61+0.06+0.00}_{-0.00-0.65-0.09-0.21}\right)\times 10^{-2},\\
&A_{CP}\left(B^0 \to K^{*0}\gamma \to K^0\pi^0\gamma\right)\\
&=\left(-0.55^{+0.37+0.68+0.43+0.03}_{-0.00-0.77-0.00-0.08}\right)\times 10^{-2},\\
&A_{CP}\left(B^+ \to K^{*+}\gamma \to K^+\pi^0\gamma\right)\\
&=\left(-0.79^{+0.24+0.37+0.79+0.18}_{-0.21-0.74-0.00-0.15}\right)\times 10^{-2},\\
&A_{CP}\left(B^+ \to K^{*+}\gamma \to K^0\pi^+\gamma\right)\\
&=\left(-0.39^{+0.35+0.70+0.02+0.46}_{-0.16-0.80-0.34-0.00}\right)\times 10^{-2},\\
&A_{CP}\left(B_s^0 \to \bar{K}^{*0}\gamma \to K^0\pi^0\gamma\right)\\
&=\left(4.22^{+0.83+0.70+0.65+0.10}_{-0.00-0.95-0.05-0.00}\right)\times 10^{-2},\\
&A_{CP}\left(B_s^0 \to \bar{K}^{*0}\gamma \to K^-\pi^+\gamma\right)\\
&=\left(4.17^{+0.00+0.52+0.00+0.00}_{-0.21-0.84-0.42-0.11}\right)\times 10^{-2},
\end{aligned} \tag{31}$$

where we find that the direct CP violations of the $B^{0,+}$ decays induced by the $b \to s$ transition are less than 1 %. For $B^{+,0}$ decays, our predictions are consistent with those of the two-body $B^{+,0} \to K^{*+,0}\gamma$ decays predicted using the PQCD approach, $A_{CP}(B^+ \to K^{*+}\gamma) = -(0.57 \pm 0.43)\times 10^{-2}$ and $A_{CP}(B^0 \to K^{*0}\gamma) = -(0.61 \pm 0.46)\times 10^{-2}$ [37], and recalculated to be $A_{CP}(B^+ \to K^{*+}\gamma) = -(0.40 \pm 0.10)\times 10^{-2}$ and $A_{CP}(B^0 \to K^{*0}\gamma) = -(0.30 \pm 0.00)\times 10^{-2}$ in Ref. [53]. On the experimental side, the direct CP asymmetries of the $B^{+,0} \to K^{*+,0}\gamma$ decays are given by the PDG [50]

$$\begin{aligned}
&A_{CP}(B^+ \to K^{*+}\gamma) = (1.4 \pm 1.8)\%,\\
&A_{CP}\left(B^0 \to K^{*0}\gamma\right) = -(0.6 \pm 1.1)\%,
\end{aligned} \tag{32}$$

where $A_{CP}(B^+ \to K^{*+}\gamma)$ is larger than 1% and opposite in sign to the PQCD predictions. Nevertheless, large errors still exist. We hope that this divergence can be clarified in future LHCb and SuperKEKB experiments by measuring the three-body B decays $B^+ \to K^{*+}\gamma \to K^+\pi^0\gamma$ and $B^+ \to K^{*+}\gamma \to K^0\pi^+\gamma$. If direct CP violation of more than a few percent is confirmed in the future, it can be considered that some new physics may contribute to these channels. Direct CP violation for B_s decays induced by the $b \to d$ transition are significantly larger than those of $B^{+,0}$ decays because the product of the CKM matrix element for the electro-magnetic penguin operator is proportional to $V_{tb}^* V_{td} \sim \lambda^3$, and that for the tree operator is either proportional to $V_{cb}^* V_{cd} \sim \lambda^3$ or $V_{ub}^* V_{ud} \sim \lambda^3$. In other words, the tree contribution is not suppressed and can be comparative with the penguin contribution. Because we know that direct CP violation arises from the interference between the tree and penguin contributions, we can expect relatively large CP asymmetries for these two B_s decays. In previous PQCD calculations [53], the authors obtained the following result:

$$A_{CP}\left(\bar{B}_s^0 \to K^{*0}\gamma\right) = \left(12.7^{+0.1+1.6+0.5}_{-0.5-2.3-0.9}\right)\times 10^{-2}, \tag{33}$$

which is indeed significantly larger than those of $B^{0,+}$ decays. Though this result is larger than our predictions, it is clear that direct CP violation for the $B_s^0 \to \bar{K}^{*0}\gamma$ decay has a positive sign, which contrasts with those of $B^{0,+} \to K^{*0,+}\gamma$ decays.

IV. SUMMARY

In this study, we analyze the three-body radiative B decays $B_{(s)} \to K^*\gamma \to K\pi\gamma$ with the $K\pi$ pair originating from the intermediate state K^* using the PQCD approach. Under the quasi-two-body-decay approximation, the $K\pi$ pair DAs are introduced, which include final-state interactions between the $K\pi$ pair in the resonant region. Both the resonant and nonresonant contributions are described by the time-like form factor $F_{K\pi}$, which is parametrized using the RBW formula for the P-wave resonance K^*. Under the condition of the narrow width approximation and isospin conservation, the branching ratios of the $B_{(s)} \to K^*\gamma \to K\pi\gamma$ decays are consistent with those of two-body $B_{(s)} \to K^*\gamma$ decays calculated in previous PQCD calculations, which verifies that the PQCD approach can be extended to three-body B decays. More importantly, our predictions are closer to data recently measured by Belle II. This indicates that it is more appropriate to study quasi-two-body B decays in the three-body framework than the two-body framework. For the decays $B_{u,d} \to K^*\gamma \to K\pi\gamma$ induced by the $b \to s$ transition, their direct CP violations are small and less than 1 %. If direct CP violation of more than a few percent is confirmed in the future, it can be considered that some new physics may contribute to these channels. For the $B_s \to K^*\gamma \to K\pi\gamma$ decays induced by the $b \to d$ transition, stronger interference exists between the tree and penguin contributions; therefore, relatively large CP asymmetries can be observed, which can be tested in the LHCb and Belle II experiments.

ACKNOWLEDGMENT

We thank Prof. Hsiang-nan Li for valuable discussions.

References

[1] J. P. Lees *et al.* (BaBar Collaboration), Phys. Rev. D **85**, 054023 (2012)
[2] J. P. Lees *et al.* (BaBar Collaboration), Phys. Rev. D **91**, 052002 (2015)
[3] C.-L. Hsu *et al.* (Belle Collaboration), Phys. Rev. D **96**, 031101 (2017)
[4] I. Adachi *et al.* (Belle Collaboration), Phys. Rev. D **100**, 011101 (2019)
[5] Y. Yusa *et al.* (Belle Collaboration), Phys. Rev. D **99**, 011102 (2019)
[6] K. H. Kang *et al.* (Belle Collaboration), Phys. Rev. D **103**, 032003 (2021)
[7] R. Aaij, *et al.* (LHCb Collaboration), Phys. Rev. Lett. **127**, 082001 (2021)
[8] R. Aaij *et al.* (LHCb Collaboration), Phys. Rev. D **90**, 112004 (2014)
[9] R. Aaij *et al.* (LHCb Collaboration), Phys. Rev. Lett. **111**, 101801 (2013)
[10] B. Bhattacharya, M. Gronau, and J. L. Rosner, Phys. Lett. B **726**, 337 (2013)
[11] M. Gronau, Phys. Lett. B **727**, 136 (2013)
[12] M. Gronau and J. L. Rosner, Phys. Rev. D **72**, 094031 (2005)
[13] D. Xu, G. N. Li, and X. G. He, Phys. Lett. B **728**, 579 (2014)
[14] G. Engelhard and G. Raz, Phys.Rev. D **72**, 114017 (2005)
[15] G. Engelhard, Y. Nir, and G. Raz, Phys.Rev. D **72**, 075013 (2005)
[16] M. Imbeault and D. London, Phys. Rev. D **84**, 056002 (2011)
[17] X. G. He, G. N. Li, and D. Xu, Phys. Rev. D **91**, 014029 (2015)
[18] S. H. Zhou, R. H. Li, Z. Y. Wei *et al.*, Phys. Rev. D **104**, 116012 (2021)
[19] S. Kränkl, T. Mannel, and J. Virto, Nucl. Phys. B **899**, 247 (2015)
[20] H. Y. Cheng, C. K. Chua, and Z. Q. Zhang, Phys. Rev. D **94**, 094015 (2016)
[21] Y. Li, Phys. Rev. D **89**, 094007 (2014)
[22] H. Y. Cheng, C. K. Chua, and A. Soni, Phys. Rev. D **76**, 094006 (2007)
[23] R. Klein, T. Mannel, J. Virtob *et al.*, JHEP **10**, 117 (2017)
[24] Z. H. Zhang, X. H. Guo, and Y. D. Yang, Phys. Rev. D **87**, 076007 (2013)
[25] C. Wang, J. B. Liu, H. n. Li *et al.*, Phys. Rev. D **97**, 034033 (2018)
[26] W. F. Wang, H. C. Hu, H. n. Li *et al.*, Phys. Rev. D **89**, 074031 (2014)
[27] W. F. Wang and H. m. Li, Phys. Lett. B **763**, 29 (2016)
[28] Z. Rui, Y. Li, and W. F. Wang, Eur. Phys. J. C **77**, 199 (2017)
[29] Y. Li, A. J. Ma, and Z. J. Xiao, Phys. Rev. D **95**, 056008 (2017)
[30] Z. Rui, Y. Li, and H. n. Li, Phys. Rev. D **98**, 113003 (2018)
[31] Y. Li, W. F. Wang, A. J. Ma *et al.*, Eur. Phys. J. C **79**, 37 (2019)
[32] Z. Q. Zhang and H. x. Guo, Eur. Phys. J. C **79**, 59 (2019)
[33] Z. T. Zou, Y. Li, and X. Liu, Eur. Phys. J. C **80**, 517 (2020)
[34] Y. Li, D. C. Yan, J. Hua *et al.*, Phys. Rev. D **104**, 096014 (2021)
[35] F. Abudin$\acute{e}$n *et al.* (Belle Collaboration), arXiv: 2110.08219[hep-ex]
[36] M. Beneke, T. Feldmann, and D. Seidel, Nucl. Phys. B **612**, 25 (2001)
[37] M. Matsumori, A. I. Sanda, and Y. Y. Keum, Phys. Rev. D **72**, 014013 (2005)
[38] A. Ali, B. Pacjak, and C. Greub, Eur. Phys. J. C **55**, 577 (2008)
[39] C. H. Chen and H. n. Li, Phys. Lett. B **561**, 258 (2003)
[40] C. H. Chen and H. n. Li, Phys. Rev. D **70**, 054006 (2004)
[41] C. H. Chen and H. n. Li, Phys. Rev. D **71**, 114008 (2005)
[42] K. M. Watson, Phys. Rev. **88**, 1163 (1952)
[43] G. Breit and E. Wigner, Phys. Rev. **49**, 519 (1936)
[44] R. Aaij *et al.* (LHCb Collaboration), Phys. Rev. D **90**, 072003 (2014)
[45] R. Aaij *et al.* (LHCb Collaboration), Phys. Rev. D **91**, 092002 (2015)
[46] T. Kurimoto, H. n. Li, and A. I. Sanda, Phys. Rev. D **65**, 014007 (2002)
[47] C. D. Lu and M. Z. Yang, Eur. Phys. J. C **28**, 515 (2003)
[48] H. n. Li, Y. L. Shen, and Y. M. Wang, JHEP **02**, 008 (2013)
[49] G. Buchalla, A. J. Buras, and M. E. Lautenbacher, Rev. Mod. Phys. **68**, 1125 (1996)
[50] P.A. Zyla *et al.* (Particle Data Group), Prog. Theor. Exp. Phys. **2020**, 083C (2020)
[51] A. Ali, G. Kramer, Y. Li *et al.*, Phys. Rev. D **76**, 074018 (2007)
[52] Y. Li, D.C. Yan, Z. Ruic *et al.*, Eur. Phys. J. C **81**, 806 (2021)
[53] W. Wang, R. H. Li, and C. D. Lu, arXiv: 0711.0432[hep-ph]